

Modeling of Molecular Flux in a Space Simulation Chamber

J. M. LABELLO,* H. S. LOWRY,† L. M. SMITH,* T. M. MOELLER,* AND
C. G. PARIGGER*

*The University of Tennessee/ UT Space Institute, Center for Laser Applications
411 B.H. Goethert Parkway, Tullahoma, TN 37388-9700, USA

†Arnold Engineering Development Complex, 1077 Schriever Ave., Arnold AFB, TN 37389-6400, USA

ABSTRACT: The method of angular coefficients is reviewed and utilized for simulation of molecular flow in vacuum systems. Mass deposition rates and molecular pumping properties of surfaces are modeled with minimal simplifications to the chamber geometry utilizing the 3D modeling software Blender. The results of the developed software are compared to analytical and Direct Simulation Monte Carlo (DSMC) predictions. Applications include predictions of ice film distributions in a space simulation chamber at the Arnold Engineering Development Complex (AEDC).

Keywords: free molecular flow, angular coefficients, cryovacuum, cryodeposits, Blender

PACS: 51.10.+y, 02.70.-c

1. INTRODUCTION

The method of angular coefficients is one of the primary means of analyzing molecular flux for the optimization of vacuum systems. However, the method can be rather involved for the analysis of complex vacuum systems as it requires consideration of various surfaces in the system. This often leads to extensive integrations needed to describe molecular flux. Simplifications are desirable to allow us to predict molecular flux distributions in a timely manner. This work describes a means of using the angular coefficients method for general vacuum chamber modeling.

Starting with the governing equations for the release and deposition of molecular flux from one surface to another, the iterative method of angular coefficients was applied to cast the problem into a matrix-vector formulation. This formulation was then incorporated into the 3-D modeling software Blender to produce a program applicable to vacuum systems with arbitrary geometry and with a user-friendly interface for data entry and visualization of results. This program, named FMFlux, has been used to model surface contamination in the 10V vacuum chamber at Arnold Engineering Development Center (AEDC). Its results have been compared to those of analytical and Direct Simulation Monte Carlo (DSMC) methods with excellent results.

2. METHOD OF ANGULAR COEFFICIENTS

A review of the angular coefficient method is presented here [1]. We assume diffuse, cosine-law scattering. As molecular flux leaves the i^{th} surface, the flux density q (molecules $cm^{-2}s^{-1}$) that arrives on the j^{th} infinitesimal surface area amounts to

$$q_{j\,arr} = -\iint \frac{q_{i\,avg} (\mathbf{s} \cdot \hat{\mathbf{n}}_i)(\mathbf{s} \cdot \hat{\mathbf{n}}_j)}{\pi s^4} dA_i, \quad (1)$$

where \mathbf{s} is the vector from dA_i to dA_j , and $\hat{\mathbf{n}}_i$ and $\hat{\mathbf{n}}_j$ are, respectively, the normal vectors of dA_i and dA_j (see Fig. 1). The arriving flux at a surface can either be adsorbed or reflected depending on the sticking coefficient, σ , of the surface. Namely,

$$q_{j_{ads}} = \sigma_j q_{j_{arr}},$$

$$q_{j_{ref}} = (1 - \sigma_j) q_{j_{arr}}. \tag{2}$$

The leaving flux density from some area is the sum of molecular flux originating from that surface area due to outgassing and the flux that is reflected from that area. Consequently, the flux density leaving the j^{th} infinitesimal area is

$$q_{j_{lvg}} = q_{j_0} - (1 - \sigma_j) \iint \frac{q_{i_{lvg}} (\mathbf{s} \cdot \hat{\mathbf{n}}_i) (\mathbf{s} \cdot \hat{\mathbf{n}}_j)}{\pi s^4} dA_i, \tag{3}$$

where q_{j_0} denotes outgassing from the j^{th} infinitesimal surface area.

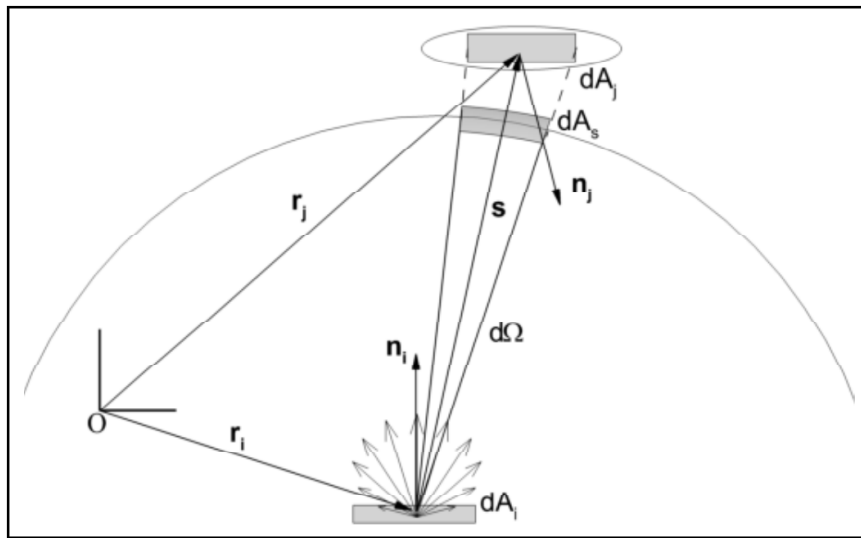


Figure 1: Geometry used to Describe the Method of Angular Coefficients using Diffuse Emission and Reflection

For non-zero $q_{j_{lvg}}$, flux can impinge upon the i^{th} surface area where it can then be reflected back to the j^{th} area. For vacuum systems with such a return flux, iterations must be performed to evaluate the steady state behavior. This is indicated by the the following iteration

$$q_{j_{lvg_{n+1}}} = q_{j_0} - (1 - \sigma_j) \iint \frac{q_{i_{lvg_n}} (\mathbf{s} \cdot \hat{\mathbf{n}}_i) (\mathbf{s} \cdot \hat{\mathbf{n}}_j)}{\pi s^4} dA_i, \tag{4}$$

where the subscript n is the iteration index.

The numerical implementation is accomplished as follows: We discretize the surfaces of a system into a number of polygonal faces so that the integral over a complex surface becomes a sum over the faces that compose that surface. Standard quadrature approach is applied in our numerical integrations. The integral over each face of a surface results in a distribution of integration points over each face of each surface in a system. In this case, Eq. 4 can be put into matrix form. Defining the matrix element

$$F_{ij} \equiv \frac{\omega_j (\sigma_i - 1)}{\pi s_{ij}^4} (\mathbf{s}_{ij} \cdot \hat{\mathbf{n}}_i) (\mathbf{s}_{ij} \cdot \hat{\mathbf{n}}_j), \tag{5}$$

where ω_j is the weight assigned to the j^{th} integration point, Eq. 4 can be written as

$$\begin{bmatrix} q_{0_{\text{ivg}_{n+1}}} \\ q_{1_{\text{ivg}_{n+1}}} \\ q_{2_{\text{ivg}_{n+1}}} \\ \vdots \\ q_{N_{\text{ivg}_{n+1}}} \end{bmatrix} = \begin{bmatrix} 0 & F_{01} & F_{02} & \dots & F_{0N} \\ F_{10} & 0 & F_{12} & \dots & F_{1N} \\ F_{20} & F_{21} & 0 & \dots & F_{2N} \\ \vdots & \vdots & \vdots & \ddots & \vdots \\ F_{N0} & F_{N1} & F_{N2} & \dots & 0 \end{bmatrix} \begin{bmatrix} q_{0_{\text{ivg}_n}} \\ q_{1_{\text{ivg}_n}} \\ q_{2_{\text{ivg}_n}} \\ \vdots \\ q_{N_{\text{ivg}_n}} \end{bmatrix} + \begin{bmatrix} q_{0_0} \\ q_{1_0} \\ q_{2_0} \\ \vdots \\ q_{N_0} \end{bmatrix}. \quad (6)$$

Here, N is the total number of integration points on every face of every surface in the system. The iteration is performed until $q_{i_{\text{ivg}_{n+1}}} - q_{i_{\text{ivg}_n}} < \varepsilon$, with ε some small, positive number.

3. INTEGRATION INTO BLENDER

Blender¹ is a free, open-source, 3D modeling software package typically used to create art, animation, and games [2]. Blender is packaged with a Python distribution that can be used for scripting. This Python distribution allows us easy access to features of Blender, including the location and orientation of faces needed to apply the method of angular coefficients. The Python program that we labeled “FMFlux” was written utilizing Eq. 6 to calculate molecular flux distributions for any geometry that can be created or imported into Blender [3].

It is important to consider whether surfaces can be totally or partially blocked when applying Eq. 6 to general three-dimensional geometries. In a free-molecular situation there will be no flux contributions between two points if the line-of-sight is blocked. This is accounted for in FMFlux by utilizing the ray-casting methods provided by Blender. By ray-casting from each point in the $N \times N$ matrix of Eq. 6 to every other point in the matrix, it can be determined which points have a clear line-of-sight and which points are blocked. For a blocked line-of-sight between any two points, a zero is substituted into the matrix in our implementation of FMFlux. This procedure can introduce errors into computation of flux contributions from partially blocked faces as the visible area of that face may be incorrectly estimated. These errors can be minimized by using more integration points per face, however, the use of more integration points increases the computational load, so the trade-off must be considered. This error is not present for completely visible or completely blocked faces.

4. RESULTS AND APPLICATIONS

A number of test cases were run to verify the accuracy of FMFlux. The considered cases include a point source depositing onto a parallel absorbing plane, a coaxial cylinder where the outer cylinder deposits onto an inner cylinder, and the 3D case of a strip source depositing onto a parallel receiving plane. Figures 2 through 5 illustrate results from these test cases. The directional point source (Fig. 2) and strip source (Figs. 4 & 5) cases are compared to analytical solutions while the coaxial cylinders (Fig. 3), which contains partially blocked faces and requires iteration, is compared to results from the 2D/axisymmetric DSMC code DS2V [4]. The (normalized) analytical solution for the point source case is given by a $F_{\text{norm}} = z^4 / (z^2 + r^2)^2$ distribution [5]. The analytical solution for the strip source case is given by Eq. 17 in Ref. [6].

The 10V space simulation chamber at AEDC has a diameter of 3 m, and a length of 10 m. This cryogenic vacuum chamber is capable of a pressure of 10^{-4} Pa ($\sim 10^{-6}$ Torr) at a temperature of 20 K. The purpose of the chamber is to test infrared sensors by providing visible and infrared scenes over a space-like spectral background [7]. One of the issues with such a cryogenic chamber is that the size and number of components in the chamber provide a multitude of possible sources for leaks and outgassing. If such sources of molecular flux are present, the

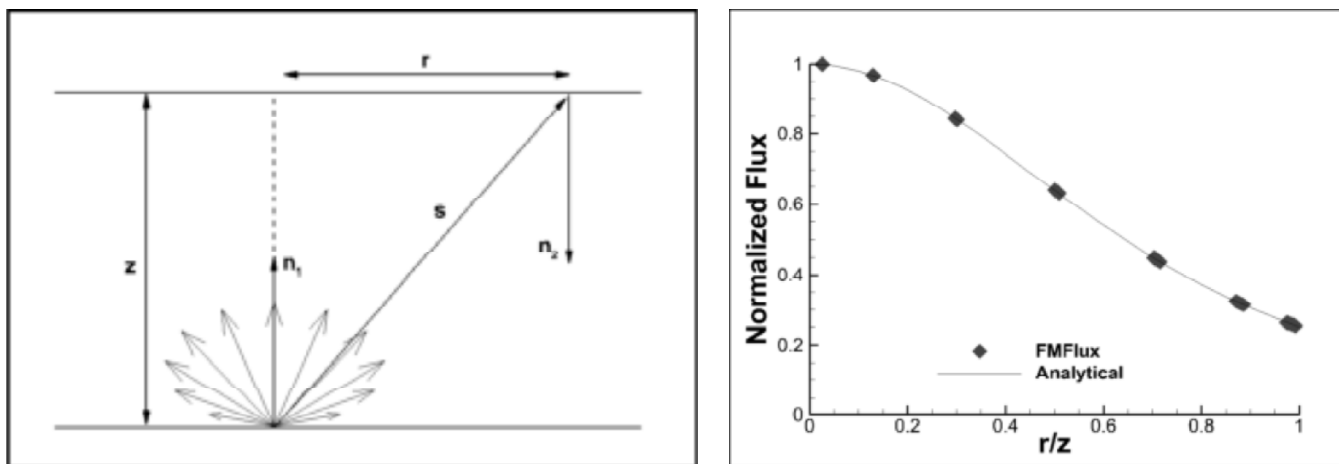


Figure 2: Geometry for flux distribution computation (left) and normalized flux on the receiving plane with the analytical result (right) using seven integration points per face per dimension

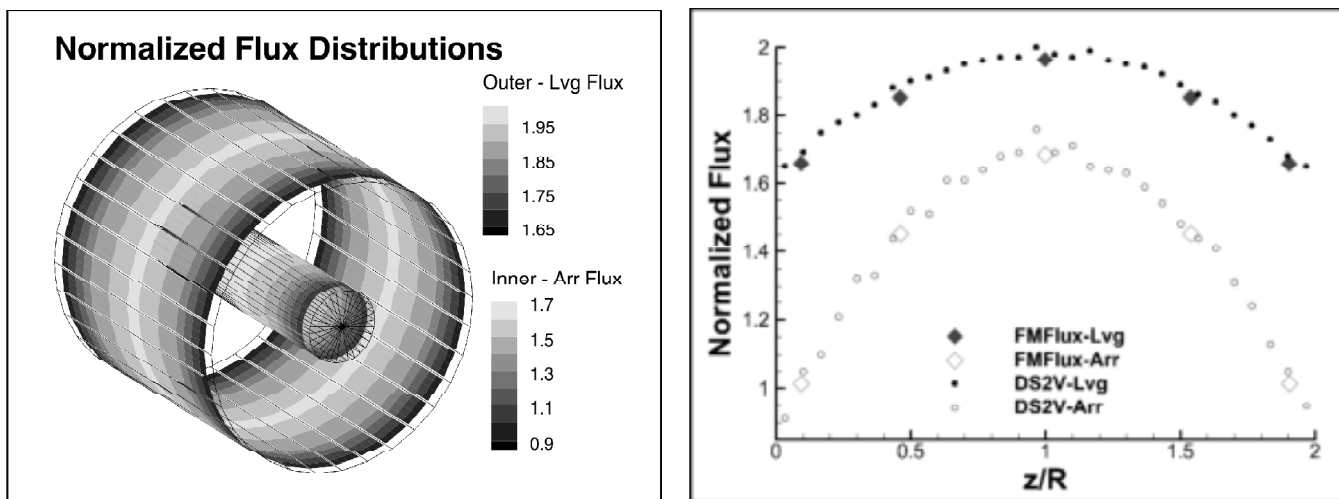


Figure 3: Results from FMFlux for coaxial cylinders (left) and flux distribution along the length of the cylinders (right) using five integration points per face per dimension. In both images, the leaving flux is shown for the outer cylinder and the arriving flux is shown for the inner cylinder. The slight discrepancy between the FMFlux result and the DSMC result for the leaving flux (right image) is due to error in calculating the visible area of partially blocked faces

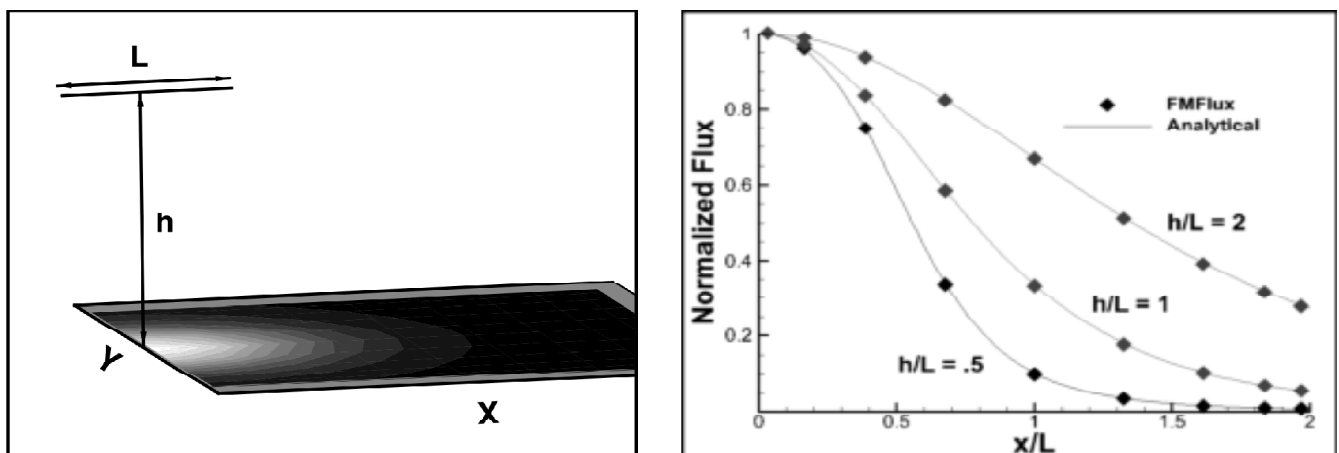


Figure 4: Geometry for the strip source case (left), and flux distribution along the x-axis of the receiving plane for several values of h/L (right)

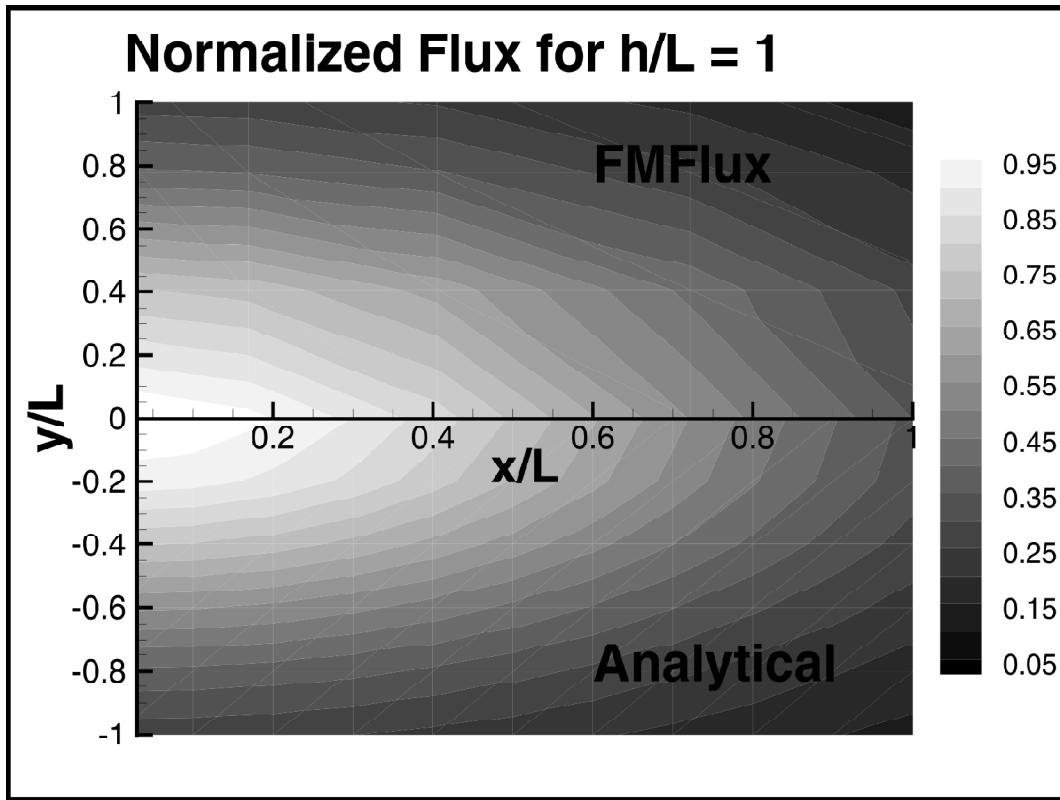


Figure 5: Comparison of flux distribution on the receiving plane of the strip source case with analytical result for $h/L = 1$

flux can deposit on the cold optics in the chamber and cause ice to build up and contaminate the system. A simple, low-polygon model of the 10V chamber was created in Blender to demonstrate the applicability of our program “FMFlux” in finding the distribution of contaminant films throughout the chamber. The simple model consists of four components: the external walls, the cryogenic shroud, a model sensor under test (SUT), and a fictitious receiving plane that is placed along the axis of the chamber. For this demonstration, the external walls were set to outgas uniformly and the sensor under test was set to outgas at ten times the rate of the walls. The sticking coefficient of the walls and the sensor was set to zero, while the cryogenic liner and the receiving plane had $\sigma = 1$. Figs. 6 through 8 illustrate the results for this model.

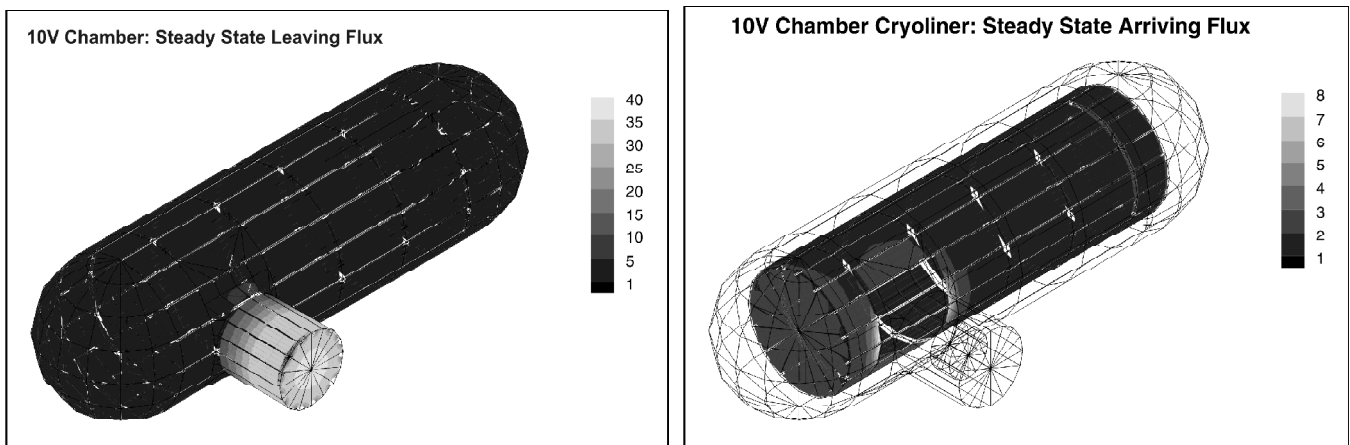


Figure 6: (Left) leaving flux distribution on the external walls of the chamber model. The walls were initially set to outgas uniformly to the interior of the chamber. (Right) arriving flux on the cryogenic shroud of the chamber is shown

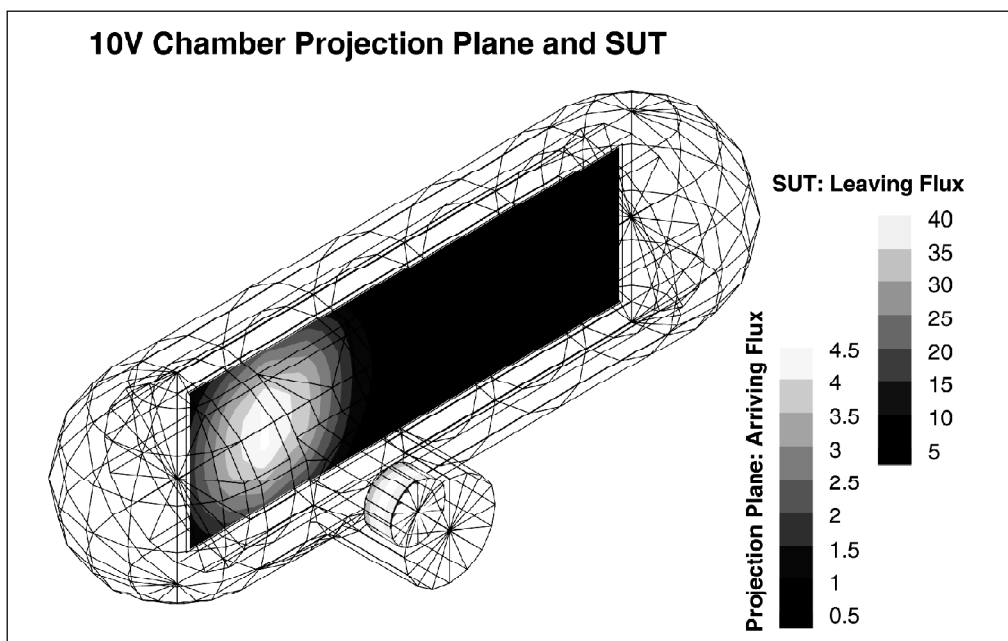


Figure 7: Leaving flux from the model sensor (a small cylinder), which was initially set to outgas uniformly at ten times the rate of the walls, and the arriving flux on the receiving plane along the axis of the chamber

Assigning a typical value of $10^{-11} \frac{g}{cm^2 s}$ for the outgassing of room temperature aluminum [8] to the external walls, the growth rate of the film on the receiving plane can be found by dividing the arriving flux density by the density of the film being deposited. Figure 8 shows the results when assuming a film density of $0.94 g/cm^3$. This is the nominal density of the low density amorphous (LDA) water ice that forms at 20 K and low pressures [9].

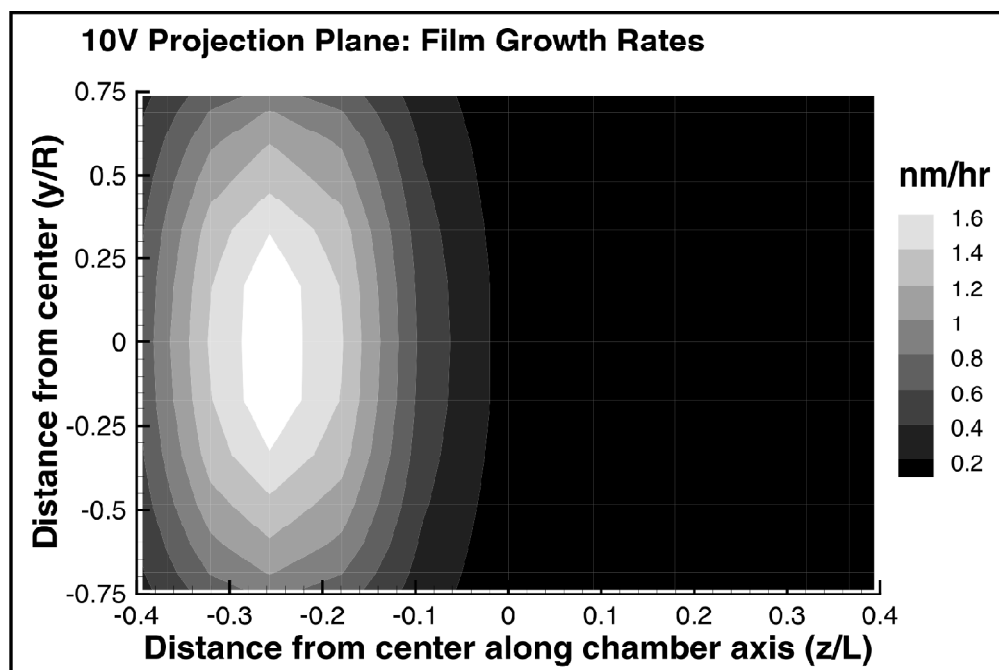



Figure 8: Growth rate of the film being deposited on the receiving plane of the simple 10V model assuming a ballpark value for outgassing from the walls and a film density of $0.94 g/cm^3$. Dimensions are normalized to the overall length, L, and radius, R, of the 10V model

5. CONCLUSION AND DISCUSSION

The method of angular coefficients has been reviewed and adapted for use in Blender [2]. This allows one to analyze flux distributions and pumping properties of complex geometries. It has been demonstrated that the program results agree well with analytic and DSMC results for the discussed cases, and the program results agree to an initial model for the entire cryogenic chamber. The work discussed here is limited to diffuse scattering; however, the method can be adapted for other reflection or emission models such as \cos^n emission often required for vacuum deposition (e.g. see [10]). The presented FMFlux incorporates the the method of angular coefficients. It can be applied to free molecular flow and requires program-input of initial outgassing rates and sticking coefficients of surfaces. These parameters are often subject to considerable uncertainty, but the method remains useful for analysis of vacuum systems [11].

Note

1.  Version 2.58a r38019, www.blender.org

References

- [1] G. Saksaganskii, *Molecular Flow in Complex Vacuum Systems*. New York: Gordon and Breach, 1988.
- [2] R. Hess, *Blender Foundations: The Essential Guide to Learning Blender 2.6*. Amsterdam: Focal Press, 2010.
- [3] J. Labello, "Water Ice Films in Cryogenic Vacuum Chambers," PhD Dissertation, The University of Tennessee, Knoxville, Tennessee, 2011.
- [4] G. A. Bird, "The DS2V/3V Program Suite for DSMC Calculations," *AIP Conference Proceedings*, **762**(1), 541–546, 2005.
- [5] M. Ohring, *Material Science of Thin Films: Deposition and Structure*, pp. 106–113. New York: Academic Press, 2nd ed., 2001.
- [6] L. Holland and W. Steckelmacher, "The Distribution of thin Films Condensed on Surfaces by the Vacuum Evaporation Method," *Vacuum*, **2**(4), 346–364, 1952.
- [7] H. Lowry, R. Nicholson, R. Simpson, K. Mead, and D. Crider, "Ground Testing of Space-based Imaging Sensors in AEDC's Space Chambers," in *24th AIAA Aerodynamic Measurement Technology and Ground Testing Conference Proceedings*, 2004.
- [8] J. Blears, E. Greer, and J. Nightingale, "Factors Determining the Ultimate Pressure in Large High-Vacuum Systems," *Advances in Vacuum Science and Technology*, pp. 473, 1960.
- [9] T. Loerting and N. Giovambattista, "Amorphous ices: Experiments and Numerical Simulations," *J. Phys.: Condens. Matter*, **18**, R919, 2006.
- [10] G. Sahu and K. Thakur, "Spatial Distribution of Copper Vapour from a Two-dimensional Source using a Strip Electron Beam at Aspect Ratio Greater than 3," *Vacuum*, **81**, 77, 2006.
- [11] A. Krasnov, "Molecular Pumping Properties of the LHC Arc Beam Pipe and Effective Secondary Electron Emission from cu surface with Artificial Roughness," *Vacuum*, **73**, 195–199, 2004.